Improving Photoplethysmographic Peak Detection through Higher-Order Interpolation Techniques

Maíssa Maniezzo[1], Italo Sandoval[1], Arthur Valencio[1], Rafael Lima[1],

[1] Samsung R&D Institute Brazil, Campinas, SP, Brazil

Abstract

Photoplethysmography (PPG) is an optical technique widely used in wearable devices for non-invasive monitoring of cardiovascular health. Nonetheless, accurate detection of PPG peaks remains a significant challenge due to noise and signal variability. This paper presents a novel approach to improve PPG peak detection through higher-order interpolation techniques. The addition of such mechanism improved accuracy, precision and recall compared to traditional and state-of-the-art peak detection algorithms such as HeartPy and Elgendi, making it a valuable contribution to the development of reliable wearable health monitoring systems.

1. Introduction

Photoplethysmogram (PPG) is a non-invasive optical technique used to measure the volumetric changes in blood flow within tissues [1]. This method involves illuminating the skin with light and measuring the amount which is absorbed or scattered by the blood vessels. The resulting signal, known as the PPG waveform, reflects the pulsatile nature of blood flow, which is driven by the cardiac cycle. The PPG signal is highly relevant to wearable health technologies, as it provides a convenient and cost-effective means of monitoring various physiological parameters, such as heart rate, blood oxygen saturation, and blood pressure [2,3], without the need for cumbersome equipment or invasive procedures.

A key feature extracted from the PPG signal is the interbeat interval (IBI), which represents the time interval between successive heartbeats [2, 3]. The IBI is traditionally calculated as the time difference in the electrocardiogram (ECG) R-peaks. However, wearable ECG technologies face limitations including high battery consumption, and susceptibility to static noise and motion. PPG signals are more commonly used in wearable devices, partially due to its simplicity and ease of implementation, but mainly due to the reduced battery consumption for continuous operation and robustness against static noise [3, 4]. Motion artifacts remain present in PPG-based technologies, but their

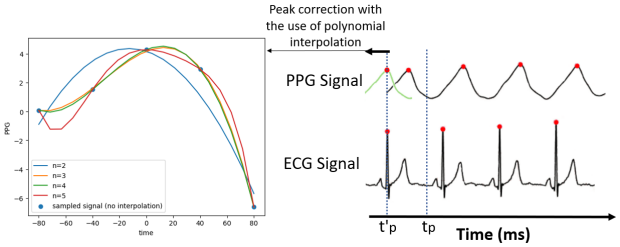


Figure 1. Fine-tuning process and objective. The goal is to reduce the distance, minimizing the Mean Squared Error (MSE), between corresponding PPG and ECG peaks along the signal through a polynomial interpolation.

effect in limb wearables - such as smartwatches and smart rings - is significantly reduced in comparison with ECG acquisitions in these areas. In the case of PPG, the IBI is determined by identifying the peaks in the PPG waveform, corresponding to the systolic phase of the cardiac cycle. The IBI value is then given by the time difference between consecutive peaks.

The importance of IBI accuracy cannot be overstated, as it impacts on the reliability and effectiveness of wearable health technologies. Inaccurate IBI measurements can lead to misdiagnosis or delayed diagnosis of cardiovascular conditions (e.g. atrial fibrillation, bradycardia), which can have serious consequences for patient outcomes. A key limitation in the accuracy of peak detection algorithms is the sampling rate of wearable PPG sensing devices (usually an order of magnitude lower than ECG devices) [3]. To overcome this limitation and estimate the best peak time, which could be between two sampled data acquisitions, interpolation strategies based on the PPG waveform can be implemented, as depicted in Figure 1. In this work we compare five interpolation strategies. In section 2, we present the concept of the interbeat interval pipeline and the interpolation strategies, including the optimization algorithms. In section 3, we compare and discuss the methodology when applied for the evaluation of a dataset of 27 subjects, at rest, wearing Samsung Galaxy Ring. Finally, in section 4, we conclude that one particular strategy, the polynomial interpolation of order 3, leads to improvements in peak detection, and, consequently, IBI compu-

tation, as presented by the increase in accuracy, precision and recall compared to other approaches.

2. Methodology

2.1. Standard IBI Framework

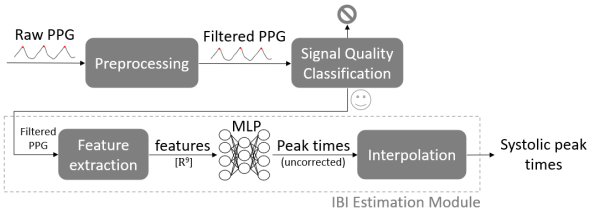


Figure 2. Diagram of a common IBI Framework.

A default IBI solution pipeline is usually composed of data preprocessing, signal quality classification and IBI estimation steps, as shown in Fig. 2. Such a pipeline is adopted, e.g., by [2, 3].

The preprocessing stage reduces noise and drifts from the collected raw PPG data by applying a bandpass filter, so the next stage receives a clearer signal focused on the frequency range consistent with the heart beat physiology.

Then, the signal quality classification stage works on detecting potentially unreliable PPG segments created due to motion and other types of noise that could reduce the quality of the IBI estimations. It works by performing a window slicing method, which classifies PPG segments as having high or low quality [5].

Regarding the IBI estimator stage, the first step is to detect all candidate peaks (pressure valleys) within the signal, e.g., using a Multi-Layer Perceptron (MLP) model. The goal of the estimator is to find samples that follow the maxima in three-point sliding windows, i.e. finding the pi where $y[p_i - 1] < y[p_i] > y[p_i + 1]$, with $y[i]$ being the amplitude of the signal in the associated i time and p_i is the candidate peak. Then, the difference between peak times is computed, producing the IBI value.

Due to low sampling frequency challenges common to several wearable devices, the IBI estimation would naturally incur in high errors, which may compromise accuracy. To reduce these errors, fine-tuning strategies can be added to the IBI estimator stage, e.g., by interpolating the peak positions, as it will be discussed next.

2.2. PPG Peak Interpolation

Fine-tuning peak positions consists of optimizing a polynomial interpolation that interprets the samples in a PPG signal segment as a polynomial curve so a more precise peak position can be calculated. The Figure 1 shows a diagram that represents this process, where the collected ECG and PPG signals (with sample rate of 500Hz and 25Hz, respectively) are not aligned, so a new peak timestamp is found to coincide with the wanted PPG peak value.

In this step, the samples given to the IBI estimator - and labeled by the MLP - get divided in segments of m samples (e.g, $m = 5$ in the definition of eqs. (3), (4) and (5)), which expresses the case when it is considered the two previous neighbor samples, the candidate peak itself (p_i) and the two following neighbor samples to the candidate peak; i.e., the samples denoted by the indices $j \in \{-2, -1, 0, 1, 2\}$. Furthermore, since the samples contain a time stamp and the amplitude of the signal in that timestamp, it can be represented by the coordinates t_{ji}, y_{ji} making it possible to construct the arrays $t_i = [t_{-2}, t_{-1}, t_0, t_1, t_2]^T - t_0$ and $y_i = [y_{-2}, y_{-1}, y_0, y_1, y_2]^T$ to each segment i.

Prior to the use of the interpolation method in the IBI solution, weights associated with the indices j are trained. The training searches for the best values for $w_i = [w_{-2}, w_{-1}, w_0, w_1, w_2]^T$, and for the relaxation parameter δ, with which the error between calculated and reference peaks is minimized. The solution undergoes optimization, defined by the problem [3]:

$$\arg\min_{W,\delta} \sum_{i \in P} [p_{i\ new} + \delta - (p_{i\ ref} - p_i)]^2 \tag{1}$$

$$[a_i, b_i, ..., z_i]^T = (X^T W X)^{-1} X^T W y_i \tag{2}$$

$$w_k > 0, \quad k \in \{-2, -1, 0, 1, 2\} \tag{3}$$

$$\sum_{k=-2}^{2} w_k = 1, \tag{4}$$

where $W = diag(w_{-2}, w_{-1}, w_0, w_1, w_2)$, $p_{i\ ref}$ is the time stamp of the ECG reference peak, p_i is the time stamp of the PPG candidate peak, and p_i new is the time stamp of the fine-tuned peak.

The structure of both p_i new and X will vary depending on the polynomial order (n) chosen for the interpolation. For the same reason, the parameters of such polynomial function are outlined as $[a_i, b_i, ..., z_i]^T$, making it an array of $n + 1$ length. Given t_s as the sampling rate, X can generally be defined as

$$X = \begin{bmatrix} -2{t_s}^n & -2{t_s}^{(n-1)} & ... & -2t_s & 1 \\ -{t_s}^n & -{t_s}^{(n-1)} & ... & -t_s & 1 \\ 0 & 0 & ... & 0 & 1 \\ {t_s}^n & {t_s}^{(n-1)} & ... & t_s & 1 \\ 2{t_s}^n & 2{t_s}^{(n-1)} & ... & 2t_s & 1 \end{bmatrix}. \tag{5}$$

As to p_i new, it can be found by solving

$$\frac{d}{dt} f(t) = 0, \tag{6}$$

where $f(t)$ is the polynomial function (order n) such as $f(t) = a_i t^n + b_i t^{n-1} + ... + y_i t + z_i$. Each of the $n - 1$

roots from equation (6) is a t point where there is a curve peak or curve valley.

To discern the intended peak, it is evaluated which root conforms to the following equation

$$\frac{d^2}{dt^2} f(t) < 0, \quad t = \{root_0, root_1, ...root_{n-1}\}. \tag{7}$$

The root found by equations (6) and (7) is the value for $p_{i\ new}$. Hence, eq. (6) is mathematically solved by:

- variable isolation, for $n = 2$;
- Bhaskara formula, for $n = 3$;
- Tartaglia formula, for $n = 4$;
- Ferrari formula, for $n = 5$.

Furthermore, the optimization described by equations (1), (2), (3) and (4) for $n = 2, 3, 4, 5$ was achieved with the use of different optimizers (e.g., Differential Evolution, Basinhopping, Curve Fit, Dual Anneling and Shgo) working on finding the global minimal of a multivariate function.

After obtaining the optimized $[w_{-2}, w_{-1}, w_0, w_1, w_2]$ values, it is now possible to apply the polynomial interpolation with trainable weights for fine-tuning the IBI solution. For example, after the detection of candidate peaks by, e.g., an MLP, the m sample segments are created as well as an Interpolation Matrix (M), defined as

$$M = (X^T W X)^{-1} X^T W, \tag{8}$$

which is used to generate the parameters for the polynomial function as described below

$$[a_i, b_i, ..., z_i] = M \cdot y_i. \tag{9}$$

The fine-tuning stage is then completed by finding the new peak time stamp - with the eqs. (6) and (7) - and using them to calculate the final peak time position, and it's signal amplitude as

$$p_{i\ final} = p_i + \delta + p_{i\ new} \tag{10}$$

$$y_{i\ final} = f(p_{i\ new}). \tag{11}$$

2.3. Evaluation Method

In the implementation for this work, we have considered a second-order Butterworth pass-band 0.8-4.5 Hz filter in the preprocessing stage, PPG segmentation of 3s in the signal quality stage, and 3 hidden layers with 1-8 neurons each and ReLU-like or logistic activation for the MLP architecture of the IBI estimation stage, with details discussed elsewhere [3, 5, 6].

The full dataset is composed of 135 volunteers's data collected at rest, split into train and test datasets in a ratio of 80% and 20%. The testing dataset contains the PPG signals of 27 volunteers using first-generation Samsung Galaxy Ring (SM-Q50X) samples, and their ECG signal for reference, collected by an GE ECG CAM-14 Acquisition Module. Each of the sessions has a duration of 35 minutes and were manually analyzed by a health specialist (cardiologist) to generate their signal quality labels for reference.

The performance of the peak detection method from the IBI solution framework is evaluated by: Accuracy, Precision, Recall and F1-score, which was calculate by defining as true positive the detection of a peak in PPG within 150 ms from a R peak in ECG. For better definition on metrics see [3]. With these metrics it is possible to build two tables: Table 1 contains the evaluations of the peak detection for $n = 2, 3, 4, 5$ and also without the interpolation step for comparison purposes; and Table 2 is the evaluation of the peak detection with weights acquired by 5 different optimizers (all working with $n = 3$). As for a baseline, four literature peak detectors were used in place of the described frameworks's peak detection stage: Elgendi [2], Heartpy library [4], Jang et al. [7], Li et al [8]. The metrics for these methods can be visualized in Table 3.

3. Results and Discussions

From Table 1 it is evidenced that the application of a fine-tuning procedure on the signal peak position improves peak detection, as given by the increase in accuracy, precision and F1 in all cases, and recall in most cases. As an example, when comparing our solution without peak interpolation and with a polynomial interpolation of order 3, an increase of 0.204% in accuracy, 0.172% in precision, 0.030% in recall, and 0.111% in F1 metrics is observed. According to the same table, the polynomial interpolation of order 3 performed better than the other orders, across all metrics as exemplified by the gain of 0.031% in accuracy, 0.020% in precision, 0.010% in recall, and 0.020% in F1 metrics when comparing it's results to the results obtained from the polynomial interpolation of order 2.

Regarding the selection of the optimizer, although Table 2 shows that the Curve Fit optimizer generated better metrics, these results were achieved only for the final test dataset, whereas prior datasets used for experiment pointed to the use of Differential Evolution optimizer. This inco-

Table 1. Metrics from Peak Detection stage with the use of Polynomial Interpolation of order n and no interpolation.

n	Optimizer	TP	FN	FP	Accuracy	Precision	Recall	F1
-	None	0.9787	0.0109	0.0104	0.9787	0.9895	0.9889	0.9891
2	Differential Evolution	0.9804	0.0107	0.0088	0.9804	0.9910	0.9891	0.9900
3	**Differential Evolution**	**0.9807**	**0.0107**	**0.0086**	**0.9807**	**0.9912**	**0.9892**	**0.9902**
4	Differential Evolution	0.9798	0.0113	0.0090	0.9798	0.9909	0.9886	0.9897
5	Differential Evolution	0.9788	0.0109	0.0103	0.9788	0.9895	0.9889	0.9892

Table 2. Metrics from Peak Detection stage using different Optimizers for weights training.

n	Optimizer	TP	FN	FP	Accuracy	Precision	Recall	F1
3	Basinhopping	0.9807	0.0107	0.0086	0.9807	0.9912	0.9892	0.9902
3	Curve Fit	0.9808	0.0107	0.0085	0.9808	0.9914	0.9892	0.9902
3	Differential Evolution	0.9807	0.0107	0.0086	0.9807	0.9912	0.9892	0.9902
3	Dual Anneling	0.9714	0.0216	0.0070	0.9714	0.9928	0.9783	0.9854
3	Shgo	0.9780	0.0115	0.0106	0.9780	0.9892	0.9883	0.9888

herence leads to believe that, even though Curve Fit optimizer may be an alternative for training polynomial interpolation's weight, Differential Evolution is a more reliable and predictable option. A second option prior to the use of Curve Fit, could be Basinhopping optimizer which has consistently generated metrics equal to the Differential Evolution ones but seemed to take more time to converge to the optimized result.

Finally, when comparing the metrics of the method in [3] with the addition of interpolation (Tables 2 and 1) with the state-of-art literature baselines (Table 3) applied to the same data, it is clear that the literature's accuracy, precision, recall and F1 values are much lower than our results. This is partially due to the specific shape of a finger PPG, with generally lower amplitude than wrist PPG, for which the solution in [3, 5, 6] has been specifically trained.

4. Conclusions

In this paper, it is proposed a novel approach to improve PPG peak detection through higher-order interpolation techniques, which can be added to a standard IBI framework. The results, summarized by Tables 1, 2 and 3 indicated that: (i) the application of a peak interpolation step improves peak detection; (ii) the best polynomial interpolation order for Galaxy Ring data is n=3; (iii) the Curve Fit, Differential Evolution, and Basinhopping are adequate optimizers; and (iv) our peak detection solution here presented has significantly higher accuracy, precision, recall, and F1 than other state-of-art peak detectors found in literature [2, 4, 7, 8].

The increase in metrics when comparing the results obtained from using a polynomial interpolation of order 3 (our best result) and 2 (suggested by [3]), despite small, may incur in significant impacts, as few missed beats (false negatives) could potentially be used by IBI applications as indicators of arrhythmia and other conditions. Besides, it is a lightweight modification requiring little additional implementation space. Given the effectiveness of the use of peak interpolation strategies, a future step is the application of other functions, e.g. a Gaussian, for this solution. Also, the presented paper limited itself to analyzing the proposed approach on the main framework used for testing (as briefly described earlier) along with a quick comparison of methods available in the public implementations of Heo et al., 2021 [9]. The decision was made due to the limited space available, however, a more profound evaluation of the approach should be conducted by applying the discussed concepts to other datasets and models, so the generalization of the conclusions can be confirmed.

Table 3. Metrics from Peak Detection stage using literature detectors.

Method	TP	FN	FP	Accuracy	Precision	Recall	F1
Elgendi	0.5212	0.4523	0.0266	0.5212	0.9515	0.5354	0.6852
Heartpy	0.8707	0.0771	0.0522	0.8707	0.9435	0.9187	0.9309
Jang	0.2541	0.7313	0.0147	0.2541	0.9455	0.2579	0.4052
Li et al.	0.7397	0.1461	0.1142	0.7397	0.8663	0.8351	0.8504

Acknowledgments

The results presented in this work were funded by Samsung Eletrônica da Amazônia Ltda., under the terms of Brazilian Informatics Law 8.248/91. The approval for human research was conceded by the organization "ConseEP Investiga" research institutes and CAAE 07327119.8.0000.5599. The authors thank Miguel C. Neves for his careful review and suggestions.

References

[1] X. Sun, P. Yang, and Y.T. Zhang. "Assessment of photoplethysmogram signal quality using morphology integrated with temporal information approach". *Annual International Conference of the IEEE Engineering in Medicine and Biology Society 2012*;2012:3456-9.

[2] M. Elgendi, "On the analysis of fingertip photoplethysmogram signals", *Current Cardiology Reviews*, vol. 8, no. 1, pp.14-25, 2012.

[3] V.B.O. Fioravanti et al, "Machine learning framework for inter-beat interval estimation using wearable photoplethysmography sensors", *Biomedical Signal Processing and Control*, vol. 88, no. A, pp. 105689, 2024.

[4] P. van Gent et al, "HeartPy: a novel heart rate algorithm for the analysis of noisy signals", *Transportation Research Part F: Traffic Psychology and Behaviour*, vol. 66, pp. 368-378, 2019.

[5] G. Lucafo et al, "Correlation-boosted ensemble local patterns for photoplethysmographic signal quality classification", *IEEE Signal Processing Letters*, vol. 32, pp. 61-65, 2025.

[6] R.G. Lima et al, "Neural architecture search for tiny detectors of inter-beat intervals", *2023 31st European Signal Processing Conference (EUSIPCO)*, pp. 1085- 1089, 2023.

[7] D.G. Jang et al, "A robust method for pulse peak determination in a digital volume pulse waveform with a wandering baseline", *IEEE Transactions on Biomedical Circuits and Systems*, vol. 8, no. 5, pp. 729-737, 2014.

[8] B.N. Li, M.C. Dong, and M.I. Vai, "On an automatic delineator for arterial blood pressure waveforms", *Biomedical Signal Processing and Control*, vol 5, no. 1, pp. 76-81, 2010.

[9] S. Heo, S. Kwon and J. Lee, "Stress detection with single PPG sensor by orchestrating multiple denoising and peak-detecting methods", *IEEE Access*, vol. 9, pp. 47777-47785, 2021.

Address for correspondence:

Arthur Lopes da Silva Valencio

Av. Cambacicas, Campinas-SP, 13097-104, Brazil

a.valencio@samsung.com